

PLANT SCIENCES

XBAT31 regulates thermoresponsive hypocotyl growth through mediating degradation of the thermosensor ELF3 in *Arabidopsis*

Lin Lin Zhang¹, Yu Jian Shao¹, Lan Ding¹, Mei Jing Wang¹, Seth Jon Davis^{2,3}, Jian Xiang Liu^{1*}

Elevated ambient temperature has wide effects on plant growth and development. ELF3, a proposed thermosensor, negatively regulates protein activity of the growth-promoting factor PIF4, and such an inhibitory effect is subjected to attenuation at warm temperature. However, how ELF3 stability is regulated at warm temperature remains enigmatic. Here, we report the identification of XBAT31 as the E3 ligase that mediates ELF3 degradation in response to warm temperature in *Arabidopsis*. XBAT31 interacts with ELF3, ubiquitinates ELF3, and promotes ELF3 degradation via the 26S proteasome. Mutation of XBAT31 results in enhanced accumulation of ELF3 and reduced hypocotyl elongation at warm temperature. In contrast, overexpression of XBAT31 accelerates ELF3 degradation and promotes hypocotyl growth. Furthermore, XBAT31 interacts with the B-box protein BBX18, and the XBAT31-mediated ELF3 degradation is dependent on BBX18. Thus, our findings reveal that XBAT31-mediated destruction of ELF3 represents an additional regulatory layer of complexity in temperature signaling during plant thermomorphogenesis.

INTRODUCTION

Global temperature increases have had major negative impacts on plant ecosystem and the productivity of crop species (1). Plants are able to sense ambient temperature changes and adjust their growth and developmental programs accordingly. In the model plant *Arabidopsis*, warm temperature alters growth, including hypocotyl elongation, leaf hyponasty, and accelerates flowering, in a process called thermomorphogenesis (2). Phytochromes, especially phyB, originally identified as photoreceptors, also function as thermosensors in *Arabidopsis* (3–5). Warm temperature accelerates the conversion of phyB from active Pfr back to inactive Pr, therefore releasing the inhibitory effects of phyB on PHYTOCHROME-INTERACTING FACTOR (PIF) family proteins, such as the basic helix-loop-helix (bHLH) transcription factor PIF4 (6). PIF4 is a key regulator of plant thermomorphogenesis, which is subjected to various regulations, both at transcriptional and posttranslational levels (7–16).

The evening complex (EC), consisting of EARLY FLOWERING3 (ELF3), ELF4, and LUX ARRHYTHMO (LUX), is a core component of the circadian clock and coordinates environmental temperature cues with endogenous developmental signals for thermoresponsive gene expression and hypocotyl growth (17). ELF3 recruits ELF4 and LUX to repress the transcriptional expression of PIF4 during early night (12, 18). ELF3 also suppresses PIF4 protein activity in an EC-independent manner by preventing PIF4 from activating its transcriptional targets in the light (19). ELF3 has a polyglutamine (polyQ) tract, and changing the length of polyQ repeats affects ELF3-dependent phenotypes in a notable and nonlinear manner (20). Recently, the polyQ repeats of ELF3 within a predicted prion-like domain (PrD) were reported to function as a thermosensor in

Arabidopsis (21). The ELF3 PrD undergoes liquid-liquid phase separation, which releases the inhibitory effect of ELF3 on PIF4 under warm temperature conditions (21); however, how the protein stability of ELF3 is controlled at warm temperature remains enigmatic.

The *Arabidopsis* B-box (BBX) protein family has one or two zinc finger BBX motifs that are important for transcriptional regulations and protein-protein interactions (22). Recently, group IV BBX proteins BBX18 and BBX23 were identified to be involved in plant thermomorphogenesis through regulating the protein abundance of ELF3 (23). Although CONSTITUTIVE PHOTOMORPHOGENIC1 (COP1), an E3 ubiquitin (Ub) ligase known to be involved in controlling ELF3 stability in the photoperiod pathway under normal temperature conditions, interacts with BBX18 and BBX23, the level of ELF3 was not found to be further increased in the *cop1-4* mutant at warm temperature, suggesting that other E3 ligases existed to regulate ELF3 degradation during plant thermomorphogenesis (23, 24). In this study, we demonstrate that XB3 ORTHOLOG 1 IN ARABIDOPSIS THALIANA, XBAT31, regulates ELF3 stability at warm temperature. Our results show that XBAT31 is a positive thermomorphogenesis regulator that interacts with ELF3 and ubiquitinates ELF3, and this leads to ELF3 degradation at warmer temperature. Full XBAT31-mediated ELF3 degradation requires the previously identified thermomorphogenesis regulator BBX18. Therefore, our findings reveal an important mechanism in which ELF3 is modulated at the protein level by XBAT31 in response to elevated ambient temperature.

RESULTS

XBAT31 regulates hypocotyl elongation at warm temperature

In our previous RNA sequencing analysis of thermoresponsive gene expression in *Arabidopsis* (23), we identified a gene-encoding putative E3 Ub protein ligase, XBAT31 (AT2G28840), that is up-regulated by warm temperature. XBAT31 is one of the five *Arabidopsis* gene products structurally related to XA21 BINDING PROTEIN3 (XB3) in rice (25–29), but its function in plants has not yet been characterized.

Copyright © 2021
The Authors, some
rights reserved;
exclusive licensee
American Association
for the Advancement
of Science. No claim to
original U.S. Government
Works. Distributed
under a Creative
Commons Attribution
NonCommercial
License 4.0 (CC BY-NC).

¹State Key Laboratory of Plant Physiology and Biochemistry, College of Life Sciences, Zhejiang University, Hangzhou 310027, China. ²Department of Biology, University of York, Heslington, York YO10 5DD, UK. ³State Key Laboratory of Crop Stress Adaptation and Improvement, School of Life Sciences, Henan University, Kaifeng 475004, China. *Corresponding author. Email: jianxiangliu@zju.edu.cn

There are two splicing isoforms of *XBAT31* in the The Arabidopsis Information Resource (TAIR) database, *XBAT31.1* and *XBAT31.2*, with *XBAT31.1* containing an additional exon. To determine which form is responsive to warm temperature, we carried out quantitative reverse transcription quantitative real-time polymerase chain reaction (RT-qPCR) in wild-type (WT) plants under conditions of normal (22°C) and warm (29°C) ambient temperatures, respectively. Compared with the expression level at normal growth temperature, the expression of *XBAT31.1*, but not *XBAT31.2*, was increased by warm temperature (Fig. 1, A and B). Therefore, we focused on *XBAT31.1* in later studies. The thermoresponsive increases in *XBAT31*

were not dependent on *PIF4* or *BBX18/BBX23* (23). We next checked the expression of *XBAT31* in *phyA* and *phyB* mutants, which are reported to function as thermosensors for hypocotyl growth (3, 4). Compared with the WT, mutation at either *PHYA* or *PHYB* or both did not substantially affect the warm temperature-induced up-regulation of *XBAT31* (fig. S1). Thus, *XBAT31* expression is responsive to warm temperature independent of *PHYA/PHYB*.

To understand the biological function of *XBAT31* in plant thermomorphogenesis, we generated several independent loss-of-function mutant lines of *XBAT31* with the CRISPR-Cas9-targeted gene editing system (fig. S2), and two of them were used for measurements

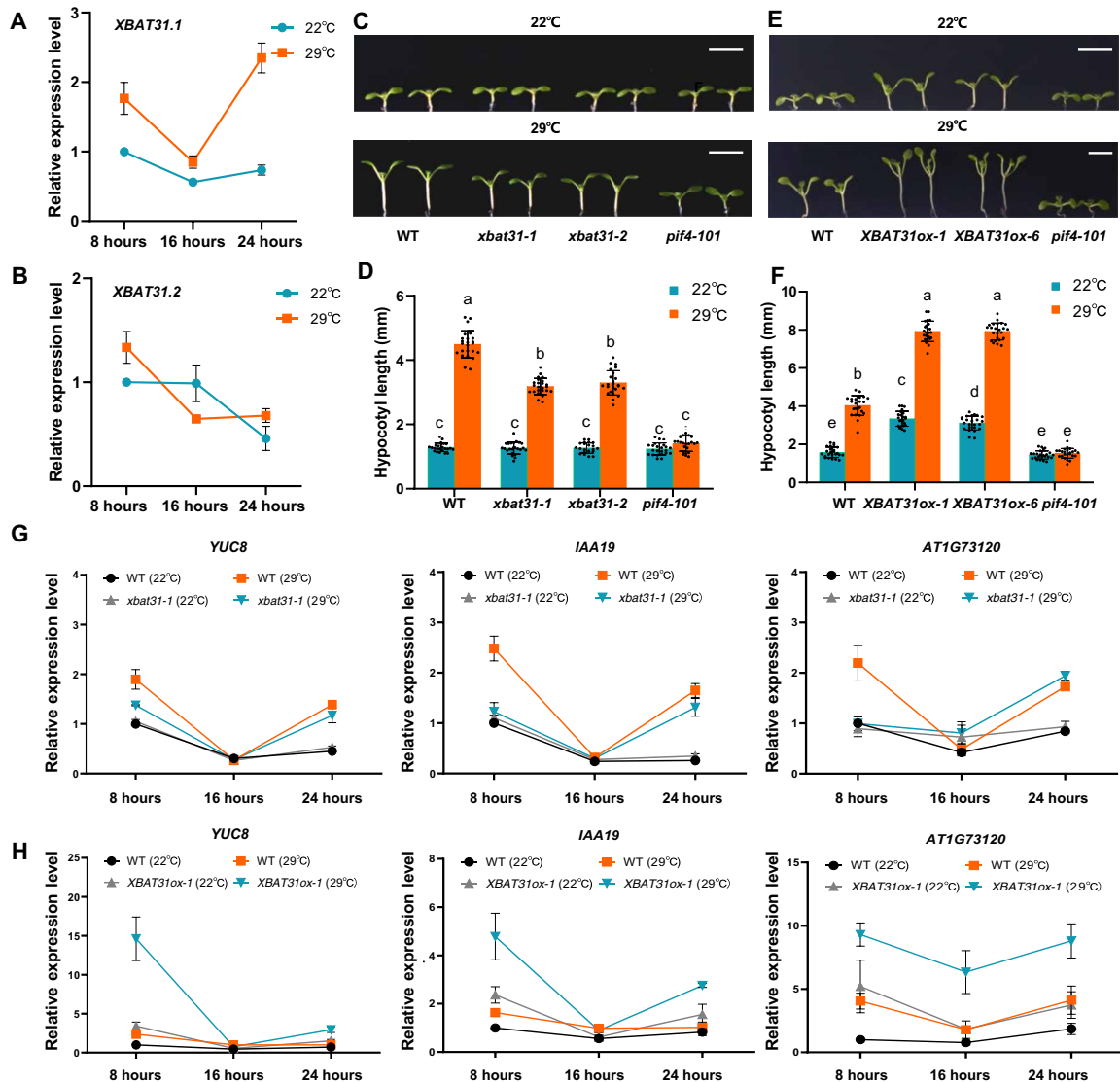


Fig. 1. *XBAT31* regulates thermomorphogenesis in *Arabidopsis*. (A and B) Regulation of *XBAT31* expression by warm temperature. Wild-type (WT) seedlings grown at 22°C were transferred to either 22° or 29°C, and then the gene expression level was examined at different Zeitgeber time (ZT) as indicated. (C to F) Phenotypes of the *XBAT31* loss-of-function mutants and *XBAT31* overexpression plants. Seedlings of the WT, gene-edited mutant (*xbat31-1/xbat31-2*), and overexpression seedlings (*XBAT31ox-1/XBAT31ox-2*) grown at 22°C were transferred to either 22° or 29°C for 3 (E and F) or 4 days (C and D), after which representative plants were imaged (C and E) and the hypocotyl length was subsequently measured (D and F). Error bars depict SD ($n = 24$). The *pif4-101* mutant was used as a control. Letters above the bars indicate significant differences as determined by post hoc test ($P < 0.05$). Scale bars, 5 mm. (G and H) Differential expression of thermoresponsive genes. WT, *xbat31-1*, and *XBAT31ox-1* plants grown at 22°C were transferred to either 22° or 29°C and then sampled at different ZT time points for gene expression analysis. The expression level of each sample was normalized to that in WT at ZT 8 hours at 22°C, which was normalized to that of *PP2A*. Error bars depict SE ($n = 3$).

of hypocotyl length, a phenotypic trait that is highly responsive to warm temperature. These mutants grew normally at the seedling stage and had a similar hypocotyl length as the WT plants under normal ambient growth temperature conditions in the light (Fig. 1, C and D) and in the dark (fig. S3, A and C). However, compared with that of the WT seedlings, the hypocotyl length was significantly reduced in both lines of *xbat31* mutants at warm temperature (Fig. 1, C and D). We next generated *XBAT31* overexpression plants using the constitutive cauliflower mosaic virus (CaMV) 35S promoter (fig. S4A). The hypocotyl length of the overexpression plants was measured, was similar to that of the WT plants in the dark (fig. S3, B and D), and was slightly longer than that in the WT plants under the light when grown at 22°C (Fig. 1, E and F). In contrast, at warm temperature (29°C), the hypocotyl length of the *XBAT31* overexpression plants was much longer than that of the WT (Fig. 1, E and F). Therefore, *XBAT31* is an important positive regulator in thermomorphogenesis in *Arabidopsis*.

Plant thermomorphogenesis often relies on transcriptional regulation of gene expression involved in phytohormone biosynthesis and signaling (8, 9, 30, 31). To further understand whether *XBAT31* controls the expression of thermoresponsive genes, we compared the expression of three auxin-responsive marker genes, *YUCCA8* (*YUC8*), *indole-3-acetic acid inducible 19* (*IAA19*), and *F-box family protein* (*AT1G73120*) (23), in the WT, *xbat31-1* mutant, and *XBAT31ox-1* overexpression plants. This was performed under both normal and warm temperature conditions. We found that all these three genes showed increased transcript accumulation in warm temperature in the WT plants at Zeitgeber time (ZT) 8 and 24 hours. However, *YUC8* displayed a lower increase, and the other two genes were not increased at warm temperature in the *xbat31-1* mutant plants at ZT 8 hours. In contrast, the expression of all these three genes was elevated by warm temperature in the *XBAT31ox-1* overexpression plants than that in the WT plants at ZT 8 and 24 hours (Fig. 1, G and H). We also checked the gene expression of *ELF3* and *PIF4*, two important genes regulating plant thermomorphogenesis. The expression of both in *xbat31-1* or *XBAT31ox-1* plants was similar to that of WT plants under both temperature conditions (fig. S5). Together, our results demonstrate that *XBAT31* is an important positive regulator of plant thermomorphogenesis.

***XBAT31* functions upstream of *PIF4* in the thermomorphogenesis pathway**

It is well established that the bHLH transcription factor *PIF4* is a hub for ambient temperature responses that integrates various environmental signals into plant morphogenesis and growth control (2). To analyze the genetic relationship between *XBAT31* and *PIF4*, we examined the hypocotyl phenotype of single mutants of *XBAT31* and *PIF4*, as well as double mutant plants under normal and warm temperature conditions. The hypocotyls of *xbat31-1 pif4-101* plants did not elongate at 29°C as much as the *pif4-101* single mutant (Fig. 2, A and D). Thus, *PIF4* is epistatic to *XBAT31*. To determine whether the function of *XBAT31* in thermomorphogenesis depends on *PIF4*, we overexpressed *XBAT31* in both the WT and *pif4-101* mutant backgrounds, obtained through genetic crossing (fig. S4B). As shown above, *XBAT31* overexpression in the WT background conferred an elevated thermoresponsive hypocotyl-growth phenotype compared with the WT. However, in the *PIF4* mutant background, *XBAT31* overexpression plants had a similar hypocotyl length as the *pif4-101* mutant plants (Fig. 2, B and E). Therefore, we concluded

that the function of *XBAT31* in hypocotyl growth is dependent on *PIF4*. Overexpression of *PIF4* in the WT background enhances hypocotyl elongation (14, 23, 32). We crossed the *PIF4* overexpression plants to the *XBAT31* mutant plants (fig. S4C) and checked the thermoresponsive hypocotyl phenotypes. As expected, *PIF4* overexpression promoted hypocotyl elongation in both the WT and *XBAT31* mutant backgrounds (Fig. 2, C and F). Together, these results support that *XBAT31* functions upstream of *PIF4* in thermomorphogenesis.

***ELF3* is epistatic to *XBAT31* during thermomorphogenesis**

ELF3 is a key component of the EC, and the EC regulates its targets in a temperature-dependent fashion (12). One of the key EC targets is the gene *PIF4* that, along with all the other EC targets, becomes more highly expressed at high temperature because *ELF3* responds to temperature, inactivating the EC (33, 34). Separately, it appears that *ELF3* also binds and inhibits the activity of the *PIF4* protein from activating its transcriptional targets (19). We were thus interested in exploring the genetic relationship of *XBAT31* and *ELF3*. Compared with the WT, *elf3-101* mutant plants had longer hypocotyls, whereas *xbat31-1* mutant plants had shorter hypocotyls at 29°C (Fig. 2, G and I). However, the *ELF3* and *XBAT31* double mutant *xbat31-1 elf3-101* plants resembled the *elf3-101* single mutant plants in terms of hypocotyl elongation (Fig. 2, G and I), which supports that *ELF3* is epistatic to *XBAT31* during thermomorphogenesis. We also generated *XBAT31* and *ELF3* double overexpression plants by crossing the *XBAT31ox-1* plants and *ELF3ox-1* plants, in which *XBAT31* and *ELF3* were overexpressed under the control of the CaMV 35S promoter (fig. S4D). *ELF3* overexpression suppressed hypocotyl elongation, while *XBAT31* overexpression promoted hypocotyl elongation at 29°C (Fig. 2, H and J). However, the hypocotyl length of the *ELF3ox-1 XBAT31ox-1* double overexpression plants was similar to that of the *XBAT31ox-1* single overexpression plants under both normal and warm temperature conditions (Fig. 2, H and J). These results suggest that the function of *XBAT31* in thermomorphogenesis is dependent on *ELF3*, and *ELF3* is probably an *in vivo* target of *XBAT31* during hypocotyl growth.

XBAT31* interacts with *ELF3*, both *in vitro* and *in vivo

To better understand the relationship between *XBAT31* and *ELF3*, we next tested for their possible protein-protein interaction in the yeast two-hybrid assay. Initial results showed that *XBAT31* interacted with *ELF3* in yeast cells; subsequently, we made four truncations (F1–F4) for *XBAT31* and three truncations (N, M, and C) for *ELF3*, respectively, to further narrow down the interaction sites (Fig. 3, A and B). It was found that the region (P301–P361) containing the RING finger domain of *XBAT31* was sufficient to interact with *ELF3*, and both the N-terminal and middle domains of *ELF3* could interact with *XBAT31* (Fig. 3, C and D).

The interactions between *XBAT31* and *ELF3* were confirmed by further assays. *In vitro* pull-down assays, the glutathione S-transferase (GST)-tagged *ELF3* precipitated with the maltose binding protein (MBP)-tagged *XBAT31* (Fig. 3E). By using split-luciferase assays and split-yellow fluorescent protein (YFP) assays in *Nicotiana benthamiana* leaves, we confirmed the occurrence of interaction between *XBAT31* and *ELF3* in plants (Fig. 3, F and G). The *XBAT31*-YFP fusion protein was observed in the nucleus (fig. S6), and the interaction between *XBAT31* and *ELF3* was also found in the nucleus in the split-YFP assays (Fig. 3G). We next performed coimmunoprecipitation (Co-IP) assays in *Arabidopsis*, and the results showed

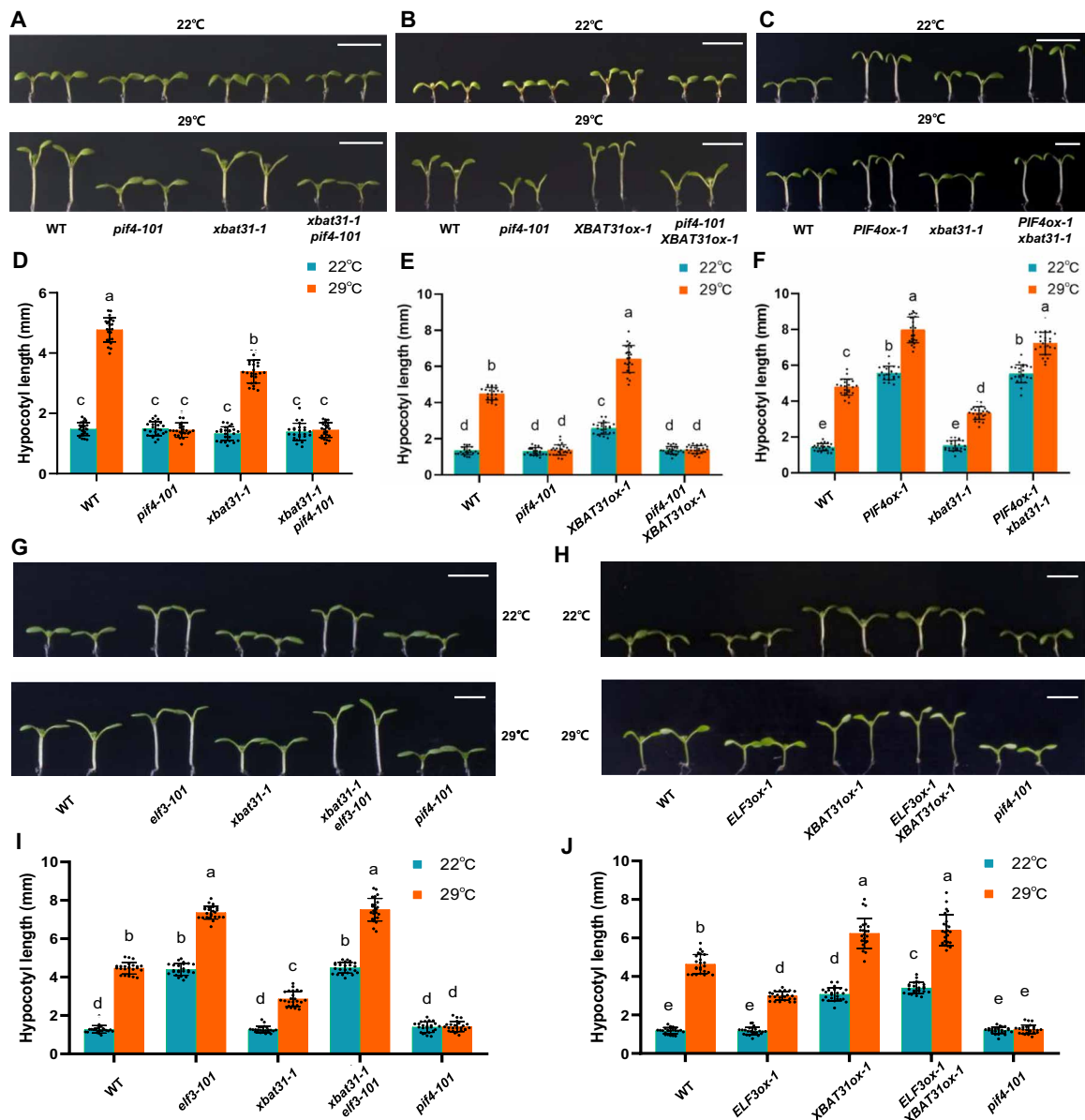


Fig. 2. Both *PIF4* and *ELF3* are epistatic to *XBAT31* in thermomorphogenesis. (A to F) Genetic analysis of *PIF4* and *XBAT31* in thermomorphogenesis. The *pif4-101* and *xbat31-1* single mutants were crossed to generate the double mutant *xbat31-1 pif4-101* (A and D), while *PIF4* was overexpressed in the *xbat31-1* mutant background by crossing the *PIF4ox-1* plants (WT background) to the *xbat31-1* plants (B and E). *XBAT31* was overexpressed in the *pif4-101* mutant background by crossing the *XBAT31ox-1* plants (WT background) to the *pif4-101* plants (C and F). (G to J) Genetic analysis between *XBAT31* and *ELF3* in thermomorphogenesis. The *XBAT31ox-1* plants (WT background) and *ELF3ox-1* (WT background) were crossed to generate the double overexpression plants (G and I), while the *xbat31-1 elf3-101* double mutant was obtained by crossing the respective single mutants (H and J). All the materials were firstly grown at 22°C and then transferred to either 22° or 29°C for 4 days, after which representative plants were imaged and the hypocotyl length was subsequently measured. Error bars depict SD ($n = 24$). The *pif4-101* mutant was used as a control. Letters above the bars indicate significant differences as determined by post hoc test ($P < 0.05$). Scale bars, 5 mm.

that the FLAG-tagged *XBAT31* could be coimmunoprecipitated with the endogenous *ELF3* (Fig. 3H). Together, our results demonstrate that *XBAT31* interacts with *ELF3*, both in vitro and in vivo.

XBAT31* mediates the ubiquitination and degradation of *ELF3

As *ELF3* is a protein that interacts with the Ub E3 ligase *XBAT31*, we speculated that *XBAT31* may negatively regulate the stability of *ELF3* by mediating its ubiquitination and degradation. To examine

whether *XBAT31* promotes this proteolysis of *ELF3*, we performed cell-free degradation assay with extracts from the WT and *XBAT31* overexpression plants, respectively. Our results showed that *ELF3* degradation was faster in *XBAT31ox-1* plants than that in WT plants. This *ELF3* degradation was inhibited by MG132, an inhibitor of the 26S proteasome degradation system (Fig. 4, A to D). Thus, *XBAT31* promotes *ELF3* degradation in a manner dependent on the 26S proteasome.

To investigate whether the E3 ligase *XBAT31* facilitates *ELF3* degradation directly by ubiquitination, we performed in vitro

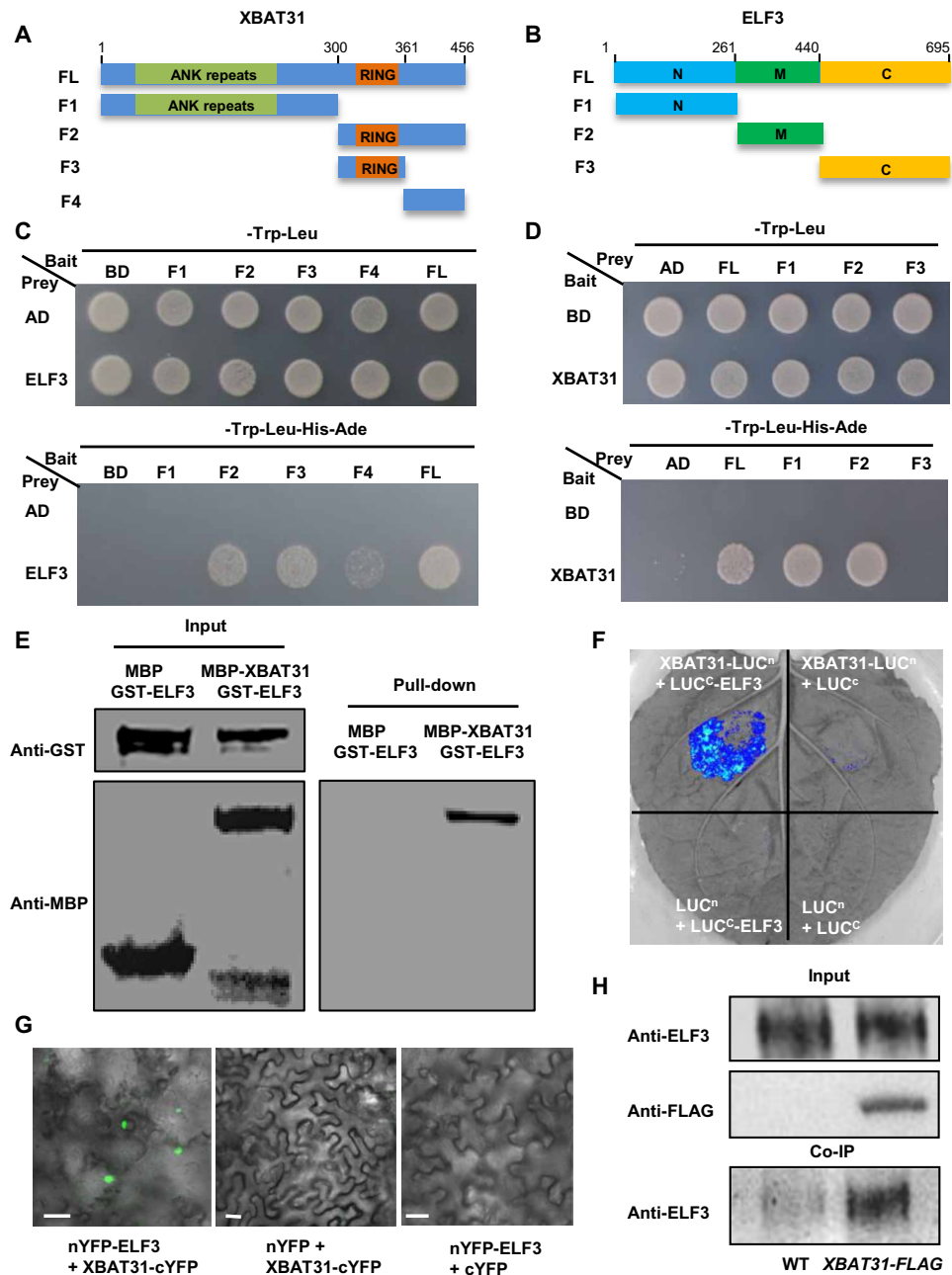


Fig. 3. XBAT31 interacts with ELF3, both in vitro and in vivo. (A to D) Protein-protein interaction between XBAT31 and ELF3 in yeast two-hybrid assays. The full-length (FL) and four truncations of XBAT31 (F1–F4) were fused with the DNA binding domain (BD), while the FL, N-terminal (N), middle (M), and C-terminal (C) regions of ELF3 were fused with the activation domain (AD) of GAL4 (A and B). *HIS3* and *ADE2* were used for interaction reporters (C and D). (E) Pull-down assay. ELF3 was fused with a GST tag, and XBAT31 was fused with an MBP tag. After coinubation with both proteins, proteins were immunoprecipitated with Glutathione-Superflow resins and detected using anti-MBP antibody. MBP was used as a negative control. (F and G) Split-luciferase and split-YFP assays. XBAT31 and ELF3 were fused with the N-terminal (nLUC) and C-terminal (cLUC) portion of firefly luciferase, or the C-terminal (cYFP) and N-terminal (nYFP) portion of YFP, respectively. Empty vectors were used as controls. Different combinations of constructs were agro-infiltrated into tobacco leaves, and the chemiluminescence or fluorescence was observed. Scale bars, 50 μ m. (H) Coimmunoprecipitation (Co-IP) assays. Equal amounts of total proteins from WT and XBAT31 overexpression (XBAT31-FLAG) plants were immunoprecipitated with FLAG antibody-conjugated beads and detected using anti-ELF3 antibody.

ubiquitination assays. GST-ELF3 and MBP-XBAT31 were purified from *Escherichia coli* and incubated in the presence or absence of E1 (UBA1), E2 (UBCh5b), and Ub. A version of XBAT31 (MBP-XBAT31M) in which the RING domain of XBAT31 was mutated (H336A) was also included. Our results showed that the native form

MBP-XBAT31, but not the mutated form MBP-XBAT31M, was auto-ubiquitinated as detected by using the anti-Ub antibody (Fig. 4E). It was difficult to differentiate the auto-ubiquitinated XBAT31 and ubiquitinated ELF3 on gels with anti-Ub antibody; however, GST-ELF3 was conjugated with Ub molecules in the presence of Ub, E1,

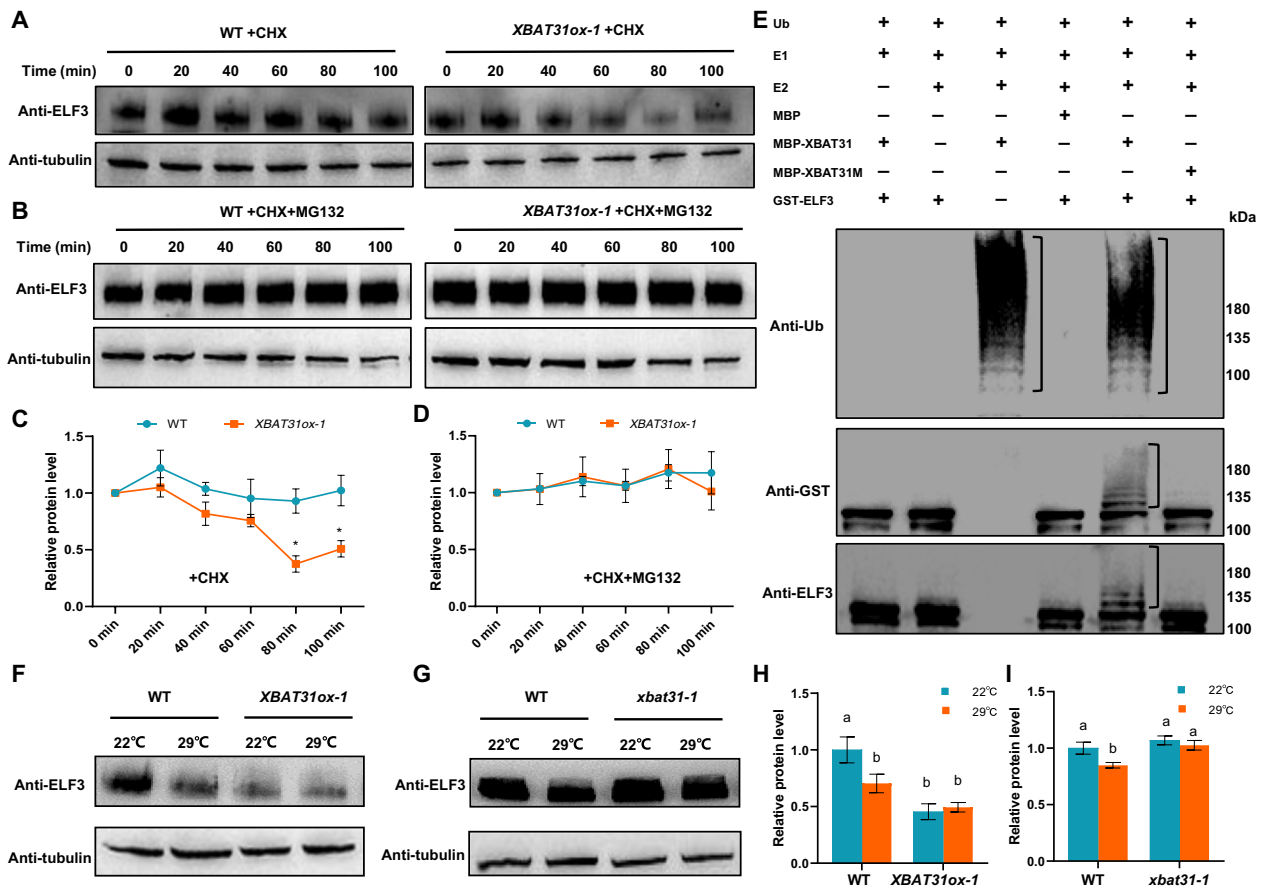


Fig. 4. XBAT31 mediates the ubiquitination and degradation of ELF3 at warm temperature. (A to D) ELF3 degradation in cell-free degradation assays. Total proteins extracted from the WT or *XBAT31* overexpression (*XBAT31ox-1*) seedlings were incubated with or without MG132 over the indicated time course, and the level of ELF3 was detected using anti-ELF3 antibody (A and B) and quantified (C and D). Tubulin was used as a loading control, and CHX was used to inhibit protein synthesis. Error bars represent SE ($n = 3$). * $P < 0.05$. (E) Ubiquitination of GST-ELF3 by XBAT31 in vitro. GST-ELF3 was incubated with the native or mutated form of MBP-XBAT31 in the presence or absence of E1, E2, and Ub. The ubiquitinated form of GST-ELF3 was detected using anti-Ub, anti-GST, and anti-ELF3 antibodies, respectively. Brackets denote the ubiquitinated bands. (F to I) Regulation of ELF3 stability by XBAT31 in vivo. WT, *XBAT31ox-1*, and *xbat31-1* seedlings grown at 22°C were transferred to 29°C, and ELF3 was checked with an anti-ELF3 antibody (F and G). Tubulin was used as a loading control. The band intensities in Western blots were quantified (H and I). Error bars represent SE ($n = 3$). Letters above the bars indicate significant differences as determined by post hoc test ($P < 0.05$). The molecular weight (kDa) of the marker is indicated on the right side of the gel.

E2, and MBP-XBAT31 as shown with the anti-GST or anti-ELF3 antibody (Fig. 4E). In contrast, the mutated form of XBAT31 (H336A) could not ubiquitinate ELF3 under the same reaction conditions (Fig. 4E). All above biochemical results demonstrate that XBAT31 can lead to the ubiquitination of ELF3, which is dependent on the RING domain of XBAT31.

To understand how XBAT31 regulates the protein stability of ELF3 in *Arabidopsis* plants during thermomorphogenesis, we examined the ELF3 protein levels by Western blotting with anti-ELF3 antibody (fig. S4G) in *XBAT31* mutant and overexpression plants under both normal and warm temperatures, respectively. Since the warm temperature-induced hypocotyl elongation was more prominent during the daytime under long-day conditions (35) and differential expression of thermoresponsive marker genes between WT and *XBAT31* mutant or overexpression plants was observed at ZT 8 hours (Fig. 1, G and H), we collected protein extracts at ZT 8 hours and performed Western blotting analysis. We found lower levels of ELF3 in the warm temperature when comparing with that at normal growth temperature in the WT (Fig. 4, F to I).

Furthermore, the protein level of ELF3 was lower in *XBAT31* overexpression plants compared with that in WT under both temperature conditions (Fig. 4, F and H). In contrast, unlike that in the WT, the ELF3 protein level was not reduced by warm temperature in the *XBAT31* mutant plants (Fig. 4, G and I). Together, our results support that XBAT31 mediates the ubiquitination and degradation of ELF3 at warm temperature.

XBAT31-mediated thermomorphogenesis requires BBX18

Previously, we have shown that the B-box family proteins BBX18 and BBX23 regulate ELF3 stability during thermomorphogenesis and that the E3 Ub ligase COP1 plays only a minor role in mediating ELF3 degradation at warm temperature (23). Therefore, we were interested in whether the function of XBAT31 in thermomorphogenesis depends on BBX18/BBX23. We crossed the *XBAT31* overexpression plants with the *BBX18* single mutant, the *BBX23* single mutant, or the double mutant *bbx18-1 bbx23-1* (fig. S4, E and F) and checked their hypocotyl growth under normal and warm temperature conditions. As reported above, overexpression of *XBAT31*

in the WT background accelerated hypocotyl elongation. However, the hypocotyl phenotype was suppressed in either the *bbx18-1* single mutant background or in the *bbx18-1 bbx23-1* double mutant background, but not in the *bbx23-1* single mutant background, both at normal and warm temperatures (Fig. 5, A to E). Our results

revealed that the function of XBAT31 in thermomorphogenesis is dependent on BBX18. We also crossed the *xbat31-1* mutant to the *bbx18-1* mutant and generated the *xbat31-1 bbx18-1* double mutant, and the phenotypic analysis showed that the hypocotyl length of the *xbat31-1 bbx18-1* double mutant is similar to that of the

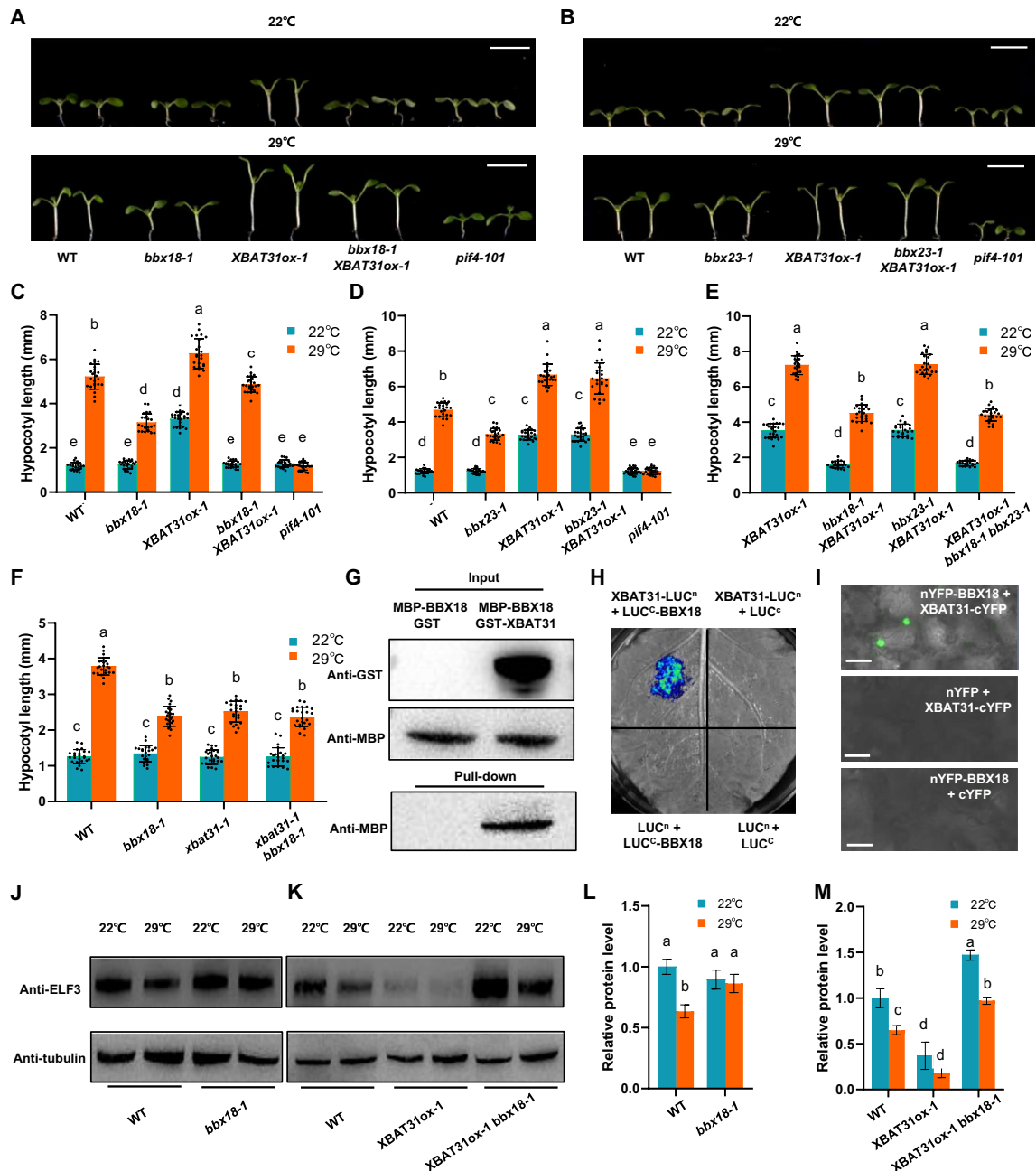


Fig. 5. XBAT31-mediated ELF3 degradation is dependent on BBX18. (A to F) Requirement of *BBX18* for *XBAT31*-mediated thermomorphogenesis. *XBAT31* overexpression plant (*XBAT31ox-1* and WT background) was crossed to the *bbx18-1*, *bbx23-1*, or *bbx18-1 bbx23-1* mutant. *xbat31-1* was also crossed to *bbx18-1*. Seedlings grown at 22°C were transferred to either 22° or 29°C for 4 days, after which representative plants were imaged (A and B). The hypocotyl length was subsequently measured (C to F). Error bars depict SD ($n = 24$). Scale bars, 5 mm. (G to I) Protein-protein interaction between *XBAT31* and *BBX18* in the pull-down assay (G), split-luciferase assay (H), and split-YFP assay (I). MBP-BBX18 and GST-XBAT31 were incubated and immunoprecipitated with Glutathione-Superflow resins and detected using anti-MBP antibody (G). Different combinations of constructs were agro-infiltrated into tobacco leaves, and the chemiluminescence or fluorescence was detected (H and I). Empty vectors were used as controls. Scale bars, 50 μm . (J to M) Dependence of *BBX18* for the *XBAT31*-regulated ELF3 stability. WT, *bbx18-1* mutant, *XBAT31ox-1*, or *XBAT31ox-1 bbx18-1* plants grown at 22°C were transferred to 29°C, and ELF3 was checked with an anti-ELF3 antibody (J and K) and quantified (L and M). Tubulin was used as a loading control. Error bars represent SE ($n = 3$). Letters above the bars indicate significant differences as determined by post hoc test ($P < 0.05$).

xbat31-1 mutant or the *bbx18-1* mutant plants (Fig. 5F). These results demonstrated that XBAT31 and BBX18 function in thermomorphogenesis in the same regulatory pathway.

To test for a possible physical interaction between XBAT31 and BBX18, we performed *in vitro* pull-down assays. Our results showed that GST-XBAT31 was able to pull down MBP-BBX18 (Fig. 5G). Split-luciferase assays and split-YFP assays further confirmed the occurrence of interaction between XBAT31 and BBX18 in plants (Fig. 5, H and I). We also checked the ELF3 protein levels at ZT 8 hours in the *XBAT31* overexpression plants in the WT and *bbx18* mutant backgrounds. As expected, the protein level of ELF3 under warm temperature conditions was higher in the *bbx18-1* mutant plants compared with that in the WT plants at ZT 8 hours (Fig. 5, J and L), and the accumulation of ELF3 in the *bbx18-1* mutant background was much higher than that in the WT background when *XBAT31* was overexpressed (Fig. 5, K and M). The ELF3 protein level was higher in the *bbx18-1* mutant background than that in the WT background at 22°C, possibly because BBX18 also has another function at normal growth temperature when *XBAT31* is overexpressed. We conclude that XBAT31-mediated degradation of ELF3 at warm temperature depends on the function of BBX18 in *Arabidopsis*.

DISCUSSION

Sensing prevailing temperature helps plant to better adapt to the surrounding environment. Both warm temperature and reduced light conditions promote hypocotyl elongation, leaf hyponasty, and early flowering. There are multiple perception points that signal thermal changes. phyB is the main photoreceptor with two different activation states (36). Warm temperature controls the conversion of phyB from the active Pfr state to the inactive Pr state, releasing the inhibitory effect of phyB on PIF4 (3, 4). In contrast, ELF3 functions in *Arabidopsis* through a differing mechanism in which warm temperature induces liquid-liquid phase separation of ELF3, leading to its inactivation and therefore activation of PIF4 at a warm temperature (21). In the current study, we demonstrate that the E3 Ub ligase XBAT31 controls the protein stability of ELF3, especially under warm temperature conditions. XBAT31-mediated thermomorphogenesis requires BBX18, a B-box family protein that responds to warm temperature, both at transcriptional and posttranslational levels (23). These results provide further insights into our understanding on how warm temperature conveys the signal to ELF3 for hypocotyl growth in plants.

The EC is a night transcriptional repressor complex that functions in the plant circadian clock and in temperature and light entrainment (12, 37, 38). Among the three core components, only LUX has a DNA binding domain and directly binds to target DNA, whereas ELF3 and ELF4 enhance the binding of EC to DNA (39). The EC represses the expression of *PIF4*, which is reduced by warm temperature (12). At warm temperature, the function of ELF4 on hypocotyl growth is dependent on *ELF3*, while overexpression of *ELF3* in *elf4-2* mutant background does not change thermal responsiveness, suggesting that these two proteins function together during thermomorphogenesis (21). However, ELF3 was also reported to function alone to inhibit the protein activity of PIF4, in which warm temperature releases such inhibitory effects (19). Genetic association studies showed that natural variation in the *ELF3* locus is correlated with warm temperature-induced hypocotyl elongation in *Arabidopsis*, supporting the role of ELF3 in controlling PIF4 activity

(33, 34). Our results showed that *XBAT31* functions upstream of *PIF4* and finely tunes the protein level of ELF3 at warm temperature. Therefore, XBAT31 regulates hypocotyl growth through releasing the inhibitory effects of ELF3 on PIF4 protein activity. We do not exclude the possibility that XBAT31 regulates thermomorphogenesis by affecting EC, since depletion of ELF3 would affect the entire EC. The expression level of *PIF4* was not markedly affected in the *XBAT31* mutant and overexpression plants in our experiments, which was probably due to the long-day conditions used in the current study.

Under normal ambient temperature conditions, ELF3 is degraded by the E3 ligase COP1 in the dark, and light diminishes the abundance of COP1 and abrogates its inhibitory effects on ELF3 and other targets to promote photomorphogenesis (24). However, warm temperature triggers the nuclear import of COP1 and alleviates the suppression of hypocotyl elongation by degrading ELONGATED HYPOCOTYL5 (HY5) (35). Both the *ELF3* transcript expression and ELF3 protein accumulation were higher at ZT 24 hours at warm temperature than that at normal ambient temperature (23). Although BBX18/BBX23 enhanced the COP1-mediated degradation of ELF3 in the effector reporter assays in tobacco leaves, mutation of *COP1* did not, while mutations of *BBX18/BBX23* did markedly affect the ELF3 accumulation during night time in *Arabidopsis* at warm temperature (23). In contrast, the *ELF3* transcriptional level was not changed, while the ELF3 protein level decreased at ZT 8 hours under light at warm temperature, and mutation of *XBAT31* was found to stabilize the ELF3 accumulation at warm temperature, while overexpression of *XBAT31* accelerated ELF3 degradation in daytime under long-day conditions, which was dependent on the function of BBX18. Therefore, XBAT31 plays a major role in controlling ELF3 stability under light at warm temperature. We do not exclude the possibility that XBAT31 and BBX18/BBX23 also function at normal ambient growth temperature, since overexpression of *XBAT31* promotes hypocotyl growth to a small extent at 22°C.

How do XBAT31 and BBX18 respond to warm ambient temperature? The expressions of both *XBAT31* and *BBX18* was increased, while the protein level of XBAT31 was not obviously affected by warm temperature. In contrast, BBX18 protein was significantly stabilized by warm temperature (23). Therefore, warm temperature may also convey signals to XBAT31 via BBX18. BBX18 belongs to the group IV BBX proteins that have two BBX motifs but lacks the CONSTANS, CO-like, and TOC1 (CCT) domain essential for the DNA binding activity in transcriptional regulation (22, 40). Although XBAT31 directly interacts with ELF3, BBX18 may function as a secondary scaffold protein to enhance the interaction between XBAT31 and ELF3 *in vivo* at warm temperature. It is not clear how warm temperature regulates the stability of BBX18, but our results indicate a central role of XBAT31 in transducing warm temperature signals from BBX18 and perhaps other BBX proteins to PIF4 in plants.

In summary, as depicted in the proposed model (Fig. 6), XBAT31 functions as a positive thermomorphogenesis regulator through regulating the protein stability of ELF3 in *Arabidopsis*. Under normal ambient growth temperatures, ELF3 suppresses PIF4 activity to inhibit hypocotyl elongation. In response to warm temperatures, both XBAT31 and BBX18 accumulate and function together to target ELF3 for 26S proteasome-associated degradation. This enables/enhances PIF4 to promote the expression of downstream genes for hypocotyl elongation, such as *YUC8*. This

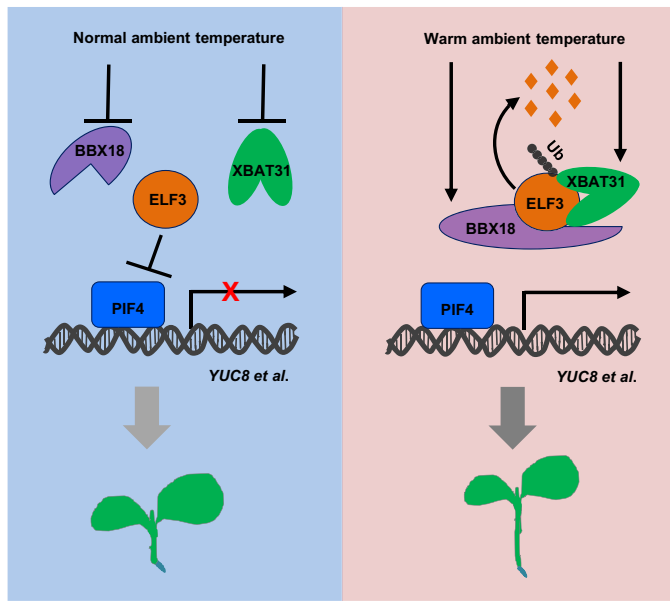


Fig. 6. A simplified working model for XBAT31-mediated thermomorphogenesis in plants. In this model, XBAT31 acts as an important regulator controlling the protein stability of ELF3 in *Arabidopsis*. Under normal ambient growth temperature conditions (e.g., 22°C), ELF3 functions as a negative regulator of PIF4 to inhibit hypocotyl elongation through either inhibiting the protein activity of PIF4 or inhibiting the expression of *PIF4*. Upon temperature elevation (e.g., 29°C), the E3 Ub ligase XBAT31 interacts, ubiquitinates, and degrades ELF3, diminishing the inhibitory effect of ELF3 on PIF4, which promotes downstream gene expression (e.g., *YUC8*) and accelerates hypocotyl elongation. The warm temperature-responsive BBX protein BBX18 possibly functions as a scaffold protein to enhance XBAT31-mediated ELF3 degradation. Since ELF3 is an important component of EC, XBAT31 may also regulate protein stability of the entire EC under warm temperature conditions.

defines XBAT31 and BBX18 as upstream regulators for thermoresponsive hypocotyl growth.

MATERIALS AND METHODS

Plant materials and hypocotyl length measurements

Plants in the Columbia-0 (Col-0) background were used in the current study. Information on *pif4-101*, *elf3-101*, *bbx18-1*, *bbx23-1*, *PIF4ox-1*, and *ELF3ox-1* plants was described in our previous paper (23). Seeds were surface sterilized with 75% ethanol for 1 min and then with 0.01% sodium hypochlorite solutions for 20 min, and subsequently washed with sterilized water. All the seeds were grown directly on half-strength Murashige and Skoog (MS) medium (containing 1.2% sucrose and 0.6% agar, pH adjusted to 5.7), stratified at 4°C for 4 days and then transferred to a standard plant incubator with the following settings: 22°C and 16/8-hour day/night.

Independent lines of *XBAT31* loss-of-function mutants were generated using the CRISPR-Cas9 system (41). For overexpression of *XBAT31*, the coding sequences (CDS) of *XBAT31.1* were amplified and inserted into pCambia1306 with the 35S promoter. Primers are included in table S1. The constructs were transformed into *Agrobacterium tumefaciens* strain GV3101 via the freeze-thaw method and introduced into *Arabidopsis* plants via the floral-dip method (42). Double mutants, double overexpression plants, and other materials as mentioned were obtained by crossing the respective parents and selecting for the appropriate segregant in the F2 generation.

For hypocotyl length measurements, when comparing the mutant plants with the WT plants, seedlings were grown at 22°C for 3 days and then transferred to 29°C or maintained at 22°C for another 4 days; when comparing the overexpression plants with the WT plants, seedlings were grown at 22°C for 4 days and then transferred to 29°C or maintained at 22°C for another 3 days. Seedlings were photographed by a camera, and the hypocotyl lengths were quantified using ImageJ software (National Institutes of Health). We used 24 seedlings from three biological replicates for these measurements. One-way analysis of variance (ANOVA) analyses and Tukey's post hoc test ($P < 0.05$) were performed for statistical analysis of the phenotypes.

Yeast two-hybrid assays

Full-length CDS and truncations of *ELF3*, *BBX18*, and *XBAT31* were cloned into pGADT7 (Clontech, Palo Alto, CA, USA) or pGBKT7 (Clontech) vectors to generate the baits and preys, respectively. Different combinations were cotransformed into yeast strain Y2HGGold (Clontech) using a commercial kit (Zymo Research, Irvine, CA, USA) and grew on selective plates at 30°C for 2 to 4 days. All the primers are listed in table S1.

Pull-down and Co-IP assays

Full-length CDS of *BBX18*, *ELF3*, and *XBAT31* was cloned into pETMALc-H or pGEX4T-1 vectors to generate MBP-BBX18, GST-ELF3, MBP-XBAT31, or GST-XBAT31 fusion proteins. Transetta cells (Novagen, Madison, WI, USA) transformed with different respective vectors were induced by isopropyl- β -D-1-thiogalactopyranoside (300 μ M) at 16°C overnight, and the resultant fusion proteins were affinity purified with either amylose agarose beads (BioLabs, London, UK) or Glutathione-Superflow resin (Takara, Japan), respectively, for MBP- and GST-tagged proteins. For pull-down assays, different combinations of recombinant proteins were incubated in pull-down buffer [20 mM Tris-HCl (pH 7.4), 200 mM NaCl, and 1 mM EDTA] for 2 hours at 4°C with slow rotations. Subsequently, the beads were washed with pull-down buffer three to five times and boiled with 2 \times SDS loading buffer. Protein extracts were separated in 4 to 20% SDS-polyacrylamide gel electrophoresis (PAGE) gels and analyzed via anti-MBP (GenScript, Piscataway, NJ, USA) or anti-GST (Abmart, Shanghai, China). For Co-IP assays, total proteins were extracted from WT and *XBAT31-FLAG* overexpression plants and immunoprecipitated with beads conjugated with anti-FLAG antibody (GenScript). After washing three times, beads were boiled with 2 \times SDS loading buffer, and Western blotting was performed with anti-ELF3 antibody (ABclonal, Wuhan, China). All the primers are listed in table S1.

Split-luciferase and split-YFP assays

Full-length CDS of *ELF3*, *BBX18*, and *XBAT31* was fused in frame with the nLUC or cLUC (23) to generate cLUC-ELF3, cLUC-BBX18, or XBAT31-nLUC. Alternatively, they were fused to the nYFP or cYFP to generate nYFP-ELF3, nYFP-BBX18, or XBAT31-cYFP. Different combinations were transformed into *A. tumefaciens* strain GV3101 and infiltrated into *N. benthamiana* leaves together with P19. Luciferase luminescence was detected by a Tanon 5200 Image Analyzer (Tanon, Shanghai, China). The YFP fluorescence signals were detected under a confocal microscope LSM710NLO (Zeiss, Oberkochen, German). All the primers are listed in table S1.

In vitro ubiquitination assays

Full-length CDS of *ELF3*, *XBAT31*, E1 (*Arabidopsis UBA1*), E2 (human *UBCH5b*), and Ub (*UBQ14*) were, respectively, cloned into pETMALc-H, pET-SUMO, or pGEX4T-1 vectors to generate GST-ELF3, MBP-XBAT31, MBP-XBAT31M, His-E1, His-E2, or His-E3 constructs that generate fusion proteins. A mutated form of *XBAT31* in the RING domain (MBP-XBAT31M, H336A) was created by overlapping PCR. These fusion proteins, as well as MBP empty control, were purified with amylose agarose (BioLabs), Ni-NTA agarose (QIAGEN, Berlin, Germany), or Glutathione-Superflow resin (Takara), respectively. Ubiquitination assays were performed in reaction buffer containing 50 mM tris-HCl (pH 7.5), 20 mM ZnCl₂, 5 mM MgCl₂, 2 mM adenosine 5'-triphosphate (ATP), 2 mM dithiothreitol (DTT), and 20 μM MG132. After 2 hours of incubation at 30°C, the reaction was stopped by adding the SDS loading buffer. Ubiquitinated GST-ELF3 was detected by using anti-Ub (Santa Cruz Biotechnology, Dallas, TX, USA), anti-GST (Abmart), and anti-ELF3 (ABclonal) antibodies, respectively.

Cell-free degradation assay

WT and *XBAT31ox-1* plants grown at 22°C under long days (LDs) for 4 days were transferred to 29°C for 3 days and sampled at ZT 8 hours. Seedlings were harvested, and total proteins were extracted using the extraction buffer [50 mM tris-MES (pH 8.0), 0.5 mM sucrose, 1 mM MgCl₂, 10 mM EDTA, and 5 mM DTT] with freshly added protease inhibitor cocktail cComplete Mini tablets (Roche, Shanghai, China). After that, the protein mixtures were incubated with 10 mM ATP and 50 μM cycloheximide (CHX) at 29°C for 0 to 100 min in the presence or absence of 50 μM MG132. After SDS-PAGE, the abundance of ELF3 was detected by Western blotting. Three independent experiments were performed, and each immunoblot was quantified using ImageJ software.

Western blot analysis

To analyze the ELF3 protein levels in WT, *XBAT31ox-1*, *xbat31-1*, *bbx18-1* plants, or the multiple mutant genotypes, seedlings grown at 22°C under LDs for 5 days were transferred to 29°C or maintained at 22°C for 24 hours and then sampled at ZT 8 hours. Total proteins were extracted with the extraction buffer [125 mM tris-HCl (pH 8.0), 375 mM NaCl, 2.5 mM EDTA, 1% SDS, and 1% β-mercaptoethanol]. Afterward, the proteins were separated in 10% SDS-PAGE gels and analyzed using anti-ELF3 (12, 19) (ABclonal, Wuhan, China) and anti-tubulin (Sigma-Aldrich, Shanghai, China) antibodies. Three independent experiments were performed, and each immunoblot was quantified using ImageJ software.

RT-qPCR

For RT-qPCR analyses, 5-day-old seedlings grown at 22°C under LDs were transferred to 29°C or maintained at 22°C for 24 hours and then sampled at ZT 8, 16, and 24 hours on the next day. Total RNAs were extracted with an RNAPrep Pure Plant kit (Tiangen, Shanghai, China). To synthesize cDNA, 2 μg of RNA and oligo (dT) primers were used in a 20-μl reaction using Moloney Murine Leukemia Virus (M-MLV) reverse transcriptase (Invitrogen, Carlsbad, CA, USA). RT-qPCR was performed with SuperReal PreMix Color (Tiangen, Shanghai, China) in accordance with the manufacturer's protocol in a CFX96 real-time system (Bio-Rad, Hercules, CA, USA). The PCR program was set as follows: first cycle, 95°C for 15 min; 40 cycles of denaturing (90°C for 10 s), annealing (60°C for 30 s), and

extension (72°C for 30 s); and last extension, 65° to 95°C for 5 s with an increment of 0.5°C. The expression level was calculated using the ΔΔCT method. There are three biological replicates in each experiment, and the expression of each gene was normalized to that of the reference gene *PP2A*. All the primers used are listed in table S1.

SUPPLEMENTARY MATERIALS

Supplementary material for this article is available at <http://advances.sciencemag.org/cgi/content/full/7/19/eabf4427/DC1>

[View/request a protocol for this paper from Bio-protocol.](#)

REFERENCES AND NOTES

1. D. B. Lobell, W. Schlenker, J. Costa-Roberts, Climate trends and global crop production since 1980. *Science* **333**, 616–620 (2011).
2. M. Quint, C. Delker, K. A. Franklin, P. A. Wigge, K. J. Halliday, M. van Zanten, Molecular and genetic control of plant thermomorphogenesis. *Nat. Plants* **2**, 15190 (2016).
3. J. H. Jung, M. Domijan, C. Klose, S. Biswas, D. Ezer, M. Gao, A. K. Khattak, M. S. Box, V. Charoensawan, S. Cortijo, M. Kumar, A. Grant, J. C. W. Locke, E. Schaefer, K. E. Jaeger, P. A. Wigge, Phytochromes function as thermosensors in *Arabidopsis*. *Science* **354**, 886–889 (2016).
4. M. Legris, C. Klose, E. S. Burgie, C. C. Rojas, M. Neme, A. Hiltbrunner, P. A. Wigge, E. Schaefer, R. D. Vierstra, J. J. Casal, Phytochrome B integrates light and temperature signals in *Arabidopsis*. *Science* **354**, 897–900 (2016).
5. Y. Qiu, M. Li, R. J. Kim, C. M. Moore, M. Chen, Daytime temperature is sensed by phytochrome B in *Arabidopsis* through a transcriptional activator HEMERA. *Nat. Commun.* **10**, 140 (2019).
6. K. J. Halliday, S. J. Davis, Light-sensing phytochromes feel the heat. *Science* **354**, 832–833 (2016).
7. M. A. Koini, L. Alvey, T. Allen, C. A. Tilley, N. P. Harberd, G. C. Whitelam, K. A. Franklin, High temperature-mediated adaptations in plant architecture require the bHLH transcription factor PIF4. *Curr. Biol.* **19**, 408–413 (2009).
8. K. A. Franklin, S. H. Lee, D. Patel, S. V. Kumar, A. K. Spartz, C. Gu, S. Ye, P. Yu, G. Breen, J. D. Cohen, P. A. Wigge, W. M. Gray, PHYTOCHROME-INTERACTING FACTOR 4 (PIF4) regulates auxin biosynthesis at high temperature. *Proc. Natl. Acad. Sci. U.S.A.* **108**, 20231–20235 (2011).
9. J. Sun, L. Qi, Y. Li, J. Chu, C. Li, PIF4-mediated activation of *YUCCA8* expression integrates temperature into the auxin pathway in regulating *Arabidopsis* hypocotyl growth. *PLOS Genet.* **8**, e1002594 (2012).
10. M. C. G. Proveniers, M. van Zanten, High temperature acclimation through PIF4 signaling. *Trends Plant Sci.* **18**, 59–64 (2013).
11. S. V. Kumar, D. Lucyshyn, K. E. Jaeger, E. Alos, E. Alvey, N. P. Harberd, P. A. Wigge, Transcription factor PIF4 controls the thermosensory activation of flowering. *Nature* **484**, 242–245 (2012).
12. D. A. Nusinow, A. Helfer, E. E. Hamilton, J. J. King, T. Imaizumi, T. F. Schultz, E. M. Farre, S. A. Kay, The ELF4-ELF3-LUX complex links the circadian clock to diurnal control of hypocotyl growth. *Nature* **475**, 398–402 (2011).
13. C. Delker, L. Sonntag, G. V. James, P. Janitza, C. Ibanez, H. Ziermann, T. Peterson, K. Denk, S. Mull, J. Ziegler, S. J. Davis, K. Schneeberger, M. Quint, The DET1-COP1-HY5 pathway constitutes a multipurpose signaling module regulating plant photomorphogenesis and thermomorphogenesis. *Cell Rep.* **9**, 1983–1989 (2014).
14. D. Ma, X. Li, Y. Guo, J. Chu, S. Fang, C. Yan, J. P. Noel, H. Liu, Cryptochrome 1 interacts with PIF4 to regulate high temperature-mediated hypocotyl elongation in response to blue light. *Proc. Natl. Acad. Sci. U.S.A.* **113**, 224–229 (2016).
15. S. N. Gangappa, S. V. Kumar, DET1 and HY5 control PIF4-mediated thermosensory elongation growth through distinct mechanisms. *Cell Rep.* **18**, 344–351 (2017).
16. L. C. van der Woude, G. Perrella, B. L. Snoek, M. van Hoogdalem, O. Novák, M. C. van Verk, H. N. van Kooten, L. E. Zorn, R. Tonckens, J. A. Dongus, M. Praat, E. A. Stouten, M. C. G. Proveniers, E. Vellutini, E. Patitaki, U. Shapulatov, W. Kohlen, S. Balasubramanian, K. Ljung, A. R. van der Krol, S. Smeekens, E. Kaiserli, M. van Zanten, HISTONE DEACETYLASE 9 stimulates auxin-dependent thermomorphogenesis in *Arabidopsis thaliana* by mediating H2A.Z depletion. *Proc. Natl. Acad. Sci. U.S.A.* **116**, 25343–25354 (2019).
17. D. Ezer, J. H. Jung, H. Lan, S. Biswas, L. Gregoire, M. S. Box, V. Charoensawan, S. Cortijo, X. Lai, D. Stöckle, C. Zubieta, K. E. Jaeger, P. A. Wigge, The evening complex coordinates environmental and endogenous signals in *Arabidopsis*. *Nat. Plants* **3**, 17087 (2017).
18. B. Thines, F. G. Harmon, Ambient temperature response establishes ELF3 as a required component of the core *Arabidopsis* circadian clock. *Proc. Natl. Acad. Sci. U.S.A.* **107**, 3257–3262 (2010).
19. C. Nieto, V. López-Salmerón, J. M. Davière, S. Prat, ELF3-PIF4 interaction regulates plant growth independently of the evening complex. *Curr. Biol.* **25**, 187–193 (2015).

20. S. F. Undurraga, M. O. Press, M. Legendre, N. Bujdoso, J. Bale, H. Wang, S. J. Davis, K. J. Verstrepen, C. Queitsch, Background-dependent effects of polyglutamine variation in the *Arabidopsis thaliana* gene *ELF3*. *Proc. Natl. Acad. Sci. U.S.A.* **109**, 19363–19367 (2012).
21. J. H. Jung, A. D. Barbosa, S. Hutin, J. R. Kumita, M. Gao, D. Derwort, C. S. Silva, X. Lai, E. Pierre, F. Geng, S.-B. Kim, S. Baek, C. Zubieta, K. E. Jaeger, P. A. Wigge, A prion-like domain in ELF3 functions as a thermosensor in *Arabidopsis*. *Nature* **585**, 256–260 (2020).
22. S. N. Gangappa, J. F. Botto, The BBX family of plant transcription factors. *Trends Plant Sci.* **19**, 460–470 (2014).
23. L. Ding, S. Wang, Z. T. Song, Y. Jiang, J. J. Han, S. J. Lu, L. Li, J. X. Liu, Two B-box domain proteins, BBX18 and BBX23, interact with ELF3 and regulate thermomorphogenesis in *Arabidopsis*. *Cell Rep.* **25**, 1718–1728.e4 (2018).
24. J. W. Yu, V. Rubio, N. Y. Lee, S. Bai, S. Y. Lee, S. S. Kim, L. Liu, Y. Zhang, M. L. Irigoyen, J. A. Sullivan, Y. Zhang, I. Lee, Q. Xie, N. C. Paek, X. W. Deng, COP1 and ELF3 control circadian function and photoperiodic flowering by regulating GI stability. *Mol. Cell* **32**, 617–630 (2008).
25. W. J. Lyzenga, J. K. Booth, S. L. Stone, The *Arabidopsis* RING-type E3 ligase XBAT32 mediates the proteasomal degradation of the ethylene biosynthetic enzyme, 1-aminocyclopropane-1-carboxylate synthase 7. *Plant J.* **71**, 23–34 (2012).
26. S. D. Carvalho, R. Saraiva, T. M. Maia, I. A. Abreu, P. Duque, XBAT35, a novel *Arabidopsis* RING E3 ligase exhibiting dual targeting of its splice isoforms, is involved in ethylene-mediated regulation of apical hook curvature. *Mol. Plant* **5**, 1295–1309 (2012).
27. H. Liu, S. Ravichandran, O. K. Teh, S. McVey, C. Lilliey, H. J. Teresinski, C. Gonzalez-Ferrer, R. T. Mullen, D. Hofius, B. Prithiviraj, S. L. Stone, The RING-type E₃ ligase XBAT_{35.2} is involved in cell death induction and pathogen response. *Plant Physiol.* **175**, 1469–1483 (2017).
28. L. A. Nodzon, W. H. Xu, Y. S. Wang, L. Y. Pi, P. K. Chakrabarty, W. Y. Song, The ubiquitin ligase XBAT32 regulates lateral root development in *Arabidopsis*. *Plant J.* **40**, 996–1006 (2004).
29. F. Yu, X. Cao, G. Liu, Q. Wang, R. Xia, X. Zhang, Q. Xie, ESCRT-I component VPS23A is targeted by E3 ubiquitin ligase XBAT35 for proteasome-mediated degradation in modulating ABA signaling. *Mol. Plant* **13**, 1556–1569 (2020).
30. W. M. Gray, A. Östin, G. Sandberg, C. P. Romano, M. Estelle, High temperature promotes auxin-mediated hypocotyl elongation in *Arabidopsis*. *Proc. Natl. Acad. Sci. U.S.A.* **95**, 7197–7202 (1998).
31. E. Oh, J. Y. Zhu, Z. Y. Wang, Interaction between BZR1 and PIF4 integrates brassinosteroid and environmental responses. *Nat. Cell Biol.* **14**, 802–809 (2012).
32. T. Yamashino, Y. Nomoto, S. Lorrain, M. Miyachi, S. Ito, N. Nakamichi, C. Fankhauser, T. Mizuno, Verification at the protein level of the PIF4-mediated external coincidence model for the temperature-adaptive photoperiodic control of plant growth in *Arabidopsis thaliana*. *Plant Signal. Behav.* **8**, e23390 (2013).
33. M. S. Box, B. E. Huang, M. Domijan, K. E. Jaeger, A. K. Khattak, S. J. Yoo, E. L. Sedivy, D. M. Jones, T. J. Hearn, A. A. R. Webb, A. Grant, J. C. W. Locke, P. A. Wigge, ELF3 controls thermoresponsive growth in *Arabidopsis*. *Curr. Biol.* **25**, 194–199 (2015).
34. A. Raschke, C. Ibañez, K. K. Ullrich, M. U. Anwer, S. Becker, A. Glöckner, J. Trenner, K. Denk, B. Saal, X. Sun, M. Ni, S. J. Davis, C. Delker, M. Quint, Natural variants of *ELF3* affect thermomorphogenesis by transcriptionally modulating *PIF4*-dependent auxin response genes. *BMC Plant Biol.* **15**, 197 (2015).
35. Y. J. Park, H. J. Lee, J. H. Ha, J. Y. Kim, C. M. Park, COP1 conveys warm temperature information to hypocotyl thermomorphogenesis. *New Phytol.* **215**, 269–280 (2017).
36. J. J. Casal, Photoreceptor signaling networks in plant responses to shade. *Annu. Rev. Plant Biol.* **64**, 403–427 (2013).
37. E. Herrero, E. Kolmos, N. Bujdoso, Y. Yuan, M. Wang, M. C. Berns, H. Uhlworm, G. Coupland, R. Saini, M. Jaskolski, A. Webb, J. Gonçalves, S. J. Davis, EARLY FLOWERING4 recruitment of EARLY FLOWERING3 in the nucleus sustains the *Arabidopsis* circadian clock. *Plant Cell* **24**, 428–443 (2012).
38. A. Helfer, D. A. Nusinow, B. Y. Chow, A. R. Gehrke, M. L. Bulyk, S. A. Kay, LUX ARRHYTHMO encodes a nighttime repressor of circadian gene expression in the *Arabidopsis* core clock. *Curr. Biol.* **21**, 126–133 (2011).
39. C. S. Silva, A. Nayak, X. Lai, S. Hutin, V. Hugouvieux, J. H. Jung, I. López-Vidriero, J. M. Franco-Zorrilla, K. C. S. Panigrahi, M. H. Nanao, P. A. Wigge, C. Zubieta, Molecular mechanisms of evening complex activity in *Arabidopsis*. *Proc. Natl. Acad. Sci. U.S.A.* **117**, 6901–6909 (2020).
40. R. Khanna, B. Kronmiller, D. R. Maszle, G. Coupland, M. Holm, T. Mizuno, S. H. Wu, The *Arabidopsis* B-box zinc finger family. *Plant Cell* **21**, 3416–3420 (2009).
41. L. Yan, S. Wei, Y. Wu, R. Hu, H. Li, W. Yang, Q. Xie, High-efficiency genome editing in *Arabidopsis* using YAO promoter-driven CRISPR/Cas9 system. *Mol. Plant* **8**, 1820–1823 (2015).
42. S. J. Clough, A. F. Bent, Floral dip: A simplified method for *Agrobacterium*-mediated transformation of *Arabidopsis thaliana*. *Plant J.* **16**, 735–743 (1998).

Acknowledgments: We thank Q. Xie and Z. He for providing the constructs of E1, E2, and Ub for the ubiquitination assays, and H. Liu and L. Wang for sharing the *phyA-211 phyB-9* mutant and *elf3-1* mutant seeds, respectively. **Funding:** This study was financially supported by grants from the National Natural Science Foundation of China (numbers 31625004, 31872653, and 32000374), the Zhejiang Provincial Talent Program (2019R52005), the Natural Science Foundation of Zhejiang, China (LD21C020001), the 111 Project (B14027), and the BBSRC (BB/N018540/1). **Author contributions:** J.X.L. and L.L.Z. conceived and designed the experiments. L.L.Z., Y.J.S., L.D., and M.J.W. performed the experiments. J.X.L. and L.L.Z. analyzed the data. J.X.L., S.J.D., and L.L.Z. wrote the article. **Competing interests:** The authors declare that they have no competing interests. **Data and materials availability:** All data needed to evaluate the conclusions in the paper are present in the paper and/or the Supplementary Materials. Additional data related to this paper may be requested from the authors.

Submitted 27 October 2020

Accepted 18 March 2021

Published 7 May 2021

10.1126/sciadv.abf4427

Citation: L. L. Zhang, Y. J. Shao, L. Ding, M. J. Wang, S. J. Davis, J. X. Liu, XBAT31 regulates thermoresponsive hypocotyl growth through mediating degradation of the thermosensor ELF3 in *Arabidopsis*. *Sci. Adv.* **7**, eabf4427 (2021).